

Innovative graph-based video processing methodology for collapse early warning of historic masonry building

Vincenzo Fioriti¹, Antonino Cataldo¹, Alessandro Colucci¹, Chiara Ormando¹, Fernando Saitta¹, Domenico Palumbo¹, Ivan Roselli¹

¹ ENEA, Casaccia Research Center, Via Anguillarese 301, 00123 Rome, Italy

ABSTRACT

In the present study an innovative video processing methodology is proposed for application to vibration data of historic masonry structures. The proposed methodology is based on graph theory and topology analysis applied to magnified videos in search of effective parameters for early-warning signals before the collapse of structures in case of earthquakes. The proposed method was validated through seismic tests of a brick-masonry mockup representing a vault of the mosque in the Palace of the Dey, Algiers. In particular, the seismic tests were carried out at increasing earthquake intensity up to the final collapse of the mockup. After processing the videos of the seismic tests by motion magnification method, the magnified video frames were transformed into a graph of the structure. Finally, several graph indices were calculated and monitored during the vibration. The monitored parameters were analyzed in search of potential threshold values suitable to generate an early warning signal. In particular, the inverse algebraic connectivity provided an early warning signal in the order of a few seconds before collapse. This was validated by comparison with an analogous signal provided at similar time by an accurate displacement lab measurements system based on optical markers positioned at several points of the tested mock-up.

Section: RESEARCH PAPER

Keywords: graph theory; early warning; topology; motion magnification; seismic test

Citation: V. Fioriti, A. Cataldo, A. Colucci, C. Ormando, F. Saitta, D. Palumbo, I. Roselli, Innovative graph-based video processing methodology for collapse early warning of historic masonry building, Acta IMEKO, vol. 13 (2024) no. 2, pp. 1-9. DOI: [10.21014/actaimeko.v13i2.1756](https://doi.org/10.21014/actaimeko.v13i2.1756)

Section Editor: Fabio Leccese, Università Degli Studi Roma Tre, Rome, Italy

Received January 31, 2024; **In final form** April 8, 2024; **Published** June 2024

Copyright: This is an open-access article distributed under the terms of the Creative Commons Attribution 3.0 License, which permits unrestricted use, distribution, and reproduction in any medium, provided the original author and source are credited.

Corresponding author: Ivan Roselli, e-mail: ivan.roselli@enea.it

1. INTRODUCTION

In recent times a variety of monitoring techniques have been developed to detect and follow the evolution of the state of damage of historic structures in order to plan proper and timely restoration and maintenance interventions. This is particularly important in areas characterized by high natural hazard, such as in seismic zones, where strong earthquakes may cause relevant structural damages up to catastrophic collapse. This is the case of many areas in the Mediterranean basin, where the presence of historic masonry buildings must coexist with a relevant probability of strong earthquakes [1].

In this context the most advanced Structural Health Monitoring (SHM) systems are essential for the protection and the conservation of the cultural heritage. SHM systems are typically designed to detect and characterise the arising and subsequent evolution of the state of damage in the structures. In general, SHM systems may provide information about a variety of parameters related to the structural state of a building,

including displacement, strain, acceleration, tensile stress, and compressive strength data [2]. In particular, most SHM methods implement vibration-based measurements using velocimeters, such as in systems based on seismographs [3], or accelerometers, like micro-electromechanical systems (MEMS) sensors, depending on the balance between cost and performance needed [4]. This approach allows to detect the dynamic response of the structure under ambient vibration excitation, providing information about the modal parameters (i.e. natural frequencies, damping ratios, mode shapes, and modal scaling factors) of the monitored building [5]. In fact, changes in the modal parameters may indicate a modification of the physical state of the structure, including the presence of damage phenomena in progress. Since also the microclimatic conditions may induce variations in the modal parameters, especially the air temperature and humidity, SHM systems should include temperature and humidity sensors [6]. For these reasons, data should be collected in different microclimatic conditions, for example, if possible, in a time span

of one year, or at least six months, in order to investigate the seasonal behaviour of the structure [6]. Anomalies or deviations from such seasonal behaviour should raise alarm and suggest deeper investigations [7]. The SHM system can be made up of a stable network of fixed sensor stations for long-term continued monitoring [8] or measurements can be performed by roving-sensors approach [3].

In the case of long-term continued monitoring stations, it is nowadays possible to install wireless sensors [9]. In recent years, the internet of things (IoT) paradigm was also applied to SHM systems, in order to improve the system's capability of processing, detecting, and transmitting data [2]. Data and information derived from data can be transmitted by internet connection and stored in a cloud before further processing steps that can be carried out by distributed systems functionalised via a big data paradigm. This allows to gather data from many locations in the monitored structure so as to obtain a mapping of the whole system, which can provide almost real-time identification and location of eventual criticalities.

In addition, lately SHM sensors are often coupled to self-sensing components made up of eco-compatible and sustainable materials (e.g. by-products or recycled materials). In this way, it is possible to develop distributed sensor networks with IoT capabilities, able to continuously gather data from remote buildings and infrastructures [10].

Moreover, it would be very useful to provide timely indications of possible imminent structural collapses, which can be used in the attempt to avoid massive death tolls and service lines failures, which may cause further disaster due to destructive fires, energy supply accidents etc. [11]. The latter is the main idea behind the concept of early warning systems. Different kinds of early warning systems can be designed for different levels of time advantage before the failure event, depending on the used sensing system and for a given hazard [12]. Present technological advances in seismic instrumentation based on accelerometers and other vibration sensors, as well as in digital communication and processing, permit the implementation of a real-time earthquake monitoring system. This is important because during earthquake events even a few second of advanced warning time can be used to activate emergency measures, such as orderly shutoff of gas pipelines or other energy lines in order to minimize fire hazard [13].

In addition, in the case of historic buildings the monitoring system should also be the least disturbing, both in terms of visual impact (e.g. to preserve the original appearance of the building) and in terms of minimum invasiveness (e.g. low-impact on the ancient materials of structural and non-structural members of walls and floors). In this context, the recent advances in the application of vision-based systems as monitoring devices are very promising [14]. Vision-based systems can solve some major drawbacks of typical conventional techniques, which usually require costly equipment set-ups for the positioning of a relatively small amount of expensive sensors (i.e. accelerometers, velocimeters etc.). As a matter of fact, the positioning of conventional contact sensors can be quite difficult, as it needs human operators physically reaching on established measuring locations [15]. On the contrary, vision-based systems are noncontact methods that permit to observe all the visible points of the structure from a distance. Consequently, it is crucial to explore the capability of extracting and analysing parameters related to structural health. In particular, it is of relevant interest to explore the potentiality of vision-based monitoring technique

to develop an earthquake-induced collapse early-warning system for historic masonry structures.

The proposed methodology is based on the analysis of video processed by the motion magnification (MM) technique through the application of the graph theory (GT) and the topological analysis (TA).

The MM is a digital video processing technique that is able to amplify the little movements of the acquired objects [16]. In brief, the MM processing algorithms detect the slight changes in pixel values along the duration of the video and infer the objects motions. Such motions can be amplified and filtered, so as to enhance specific modes of vibration. In a recent work, the advantages in the use of MM videos in comparison to conventional SHM techniques for the study of historic buildings were pointed out [17].

Moreover, the pixels corresponding to a given structure in a video frame can be assumed as a series of points linked to each other by mechanical properties. A possible representation of those points can be mathematically expressed as a graph object. As a consequence, the resulting graph is a representation of the studied object, whose mechanical deformations can be studied in terms of graph properties of nodes and links (or edges). The graph theory provides specific laws and parameters to express the inter-relations between nodes and links [18], [19]. In the graph theory, the geometrical deformations that do not substantially change the shape of the overall object (homeomorphisms) are studied by the so-called topology [20], [21]. In particular, some topological invariant properties can be defined if they are invariant with respect to the deformations of the object.

The proposed method was validated through an experimental program of earthquakes reproduced by shaking table testing of a mock-up representing a typical historic masonry structure. The videos acquired during the seismic test were magnified by the phase-based MM algorithm. Afterwards, each frame extracted from the magnified videos was transformed into a graph, and finally processed by GT and TA tools.

It is expected that, as the damage level in the structure proceeds, the overall structural deformation or dynamic behaviour parameters could provide some kind of anomalous signals usable for early warning purposes. In general, cracks and deformations in the structures slowly arise and develop until the failure. They can be monitored by contact sensors through conventional SHM systems. The proposed methodology explored the possibility of detection the effects of such deformations by non-contact equipment in term of anomalous signals in the graph parameters. Consequently, the experimental results were analysed in the attempt to find out whether some graph parameters are able to provide any anomalous values before the final activation of the structural collapse. The detection of such anomalous values in the graph parameters was validated by comparison with signal in a 3D motion capture system, called 3D Vision system, capable of an accurate monitoring of structural damage through the displacements measurement of hundreds of markers on the tested mock-ups in the laboratory seismic tests [22].

It is also crucial to understand the obtainable advance timing of the anomalous signals to be used in the early warning system. Of course, a few seconds before structural failure does not constitute a significant warning timing for people evacuation. Nonetheless, it is a sufficient time advance to activate properly designed safety systems and/or to interrupt/isolate energy lines so as to avoid further disastrous consequences.

2. METHODS

2.1. Motion Magnification of videos

The first step of the proposed methodology consists in the application of the MM method to the acquired videos of the structure. MM is based on algorithms that are able to amplify the movements of the pixels in the digital videos, even if such movements are hardly visible to the naked eye, while keeping the objects topology. When studying motions related to vibrations it is extremely useful that in the MM algorithms a frequency range of interest can be chosen.

Several MM algorithms are currently available. They have different characteristics, but they all have in common the capability to process the pixel intensity values in the attempt to reconstruct the objects motion with magnified amplitude. Such possibilities are theoretically not new. But only in recent years the main problems related to low video frame rate and resolution, as well as the large computing time required for processing real digital video footages were solved in a manner to obtain reasonably good results. Also, the development of more effective MM algorithms helped in obtaining final analysis in a reasonably short elaboration time, which is particularly important for implementing real-time or quasi real-time early warning systems.

The Eulerian version of the algorithm, also known as Eulerian Video Magnification (EVM) [23], will be considered in the following. EVM amplifies the I values similarly to an optical flow that changes at a fixed pixel position. On the one hand, EVM approach can considerably reduce the computing resources and time required. On the other hand, in EVM high values of the magnification factor a cannot be applied to high-frequency motion, while the noise rises linearly with the magnification factor. Consequently, the EVM was further developed to overcome such issues and a new version of the MM algorithms was suggested by [24] applying a complex steerable pyramid in the Eulerian framework. This version was called phase-based Motion Magnification (PBMM). In PBMM version the pixel intensity is decomposed in wavelets, whose phase difference between frames is amplified to magnify the object displacements.

Generally speaking, let's assume that a digital video is a temporal sequence of frames made up of pixels, whose intensity I depends on the pixel position (x, y) in the image and on the time t . In the following, for simplicity only the x coordinate will be considered to describe the mono-dimensional translation of pixels due to a displacement $\delta(t)$ in the video. Obviously, also the composition of motion in the y direction should be considered, but it will not be treated here.

According to the above assumptions and formulation of the MM procedure, the basic formula to express the variation of I magnified by the magnification factor α can be written as follows:

$$\Delta I = f(x - (1 + \alpha) \delta(t)). \quad (1)$$

Under the assumption that the displacement $\delta(t)$ is small enough to be approximated in terms of the Taylor's first order series around x at the time t , then $I(x, t)$ is as follows:

$$I(x, t) = f(x) - \delta(t) \left(\frac{\partial f}{\partial x} \right) + \varepsilon, \quad (2)$$

where ε is the error in the Taylor's approximation. Consequently, at each pixel variation of I can be written as follows:

$$\Delta I = I(x, t) - I(x, 0). \quad (3)$$

Assuming also that ΔI can be approximately considered as proportional to the real object displacement, then the magnified intensity I_m can be calculated as follows:

$$I_m(x, t) \approx f(x) - (1 + \alpha) \delta(t) \left(\frac{\partial f}{\partial x} \right), \quad (4)$$

As equation (4) was calculated through a band-pass derivation, then the magnified motion displacement is essentially obtained by simply adding $\alpha \Delta(x, t)$ to $I(x, t)$. The validity of the above assumption is related to the validity of the Taylor's expansion, which means that the error ε and the amplification factor α must remain sufficiently small so that the algorithm works within a linearity bound. As a consequence, the computational resources and time required could be relevant. This might represent a major problem of the processing procedure, especially if the video duration is very long and/or the pixel resolution is very high.

Another obvious limitation of the MM algorithm is represented by the frame rate of the processed video. In fact, the frame rate (generally expressed in frames-per-second, fps) represents the sampling frequency of the acquired data. According to the Nyquist sampling theorem, the maximum frequency of interest (f_{\max}) that can be analysed is the half value of the fps speed of acquisition. This has a major implication in the study of vibrating objects, like in the case of earthquake monitoring. For instance, considering that most common video camera acquire at around 30 fps, then the highest frequency of the studied object that can be analysed is $f_{\max} = 15$ Hz [25]. However, it is well known that in the study of vibrating objects it is necessary to apply abundant oversampling (at least 5 if not 10 times the f_{\max}), which means that it is very hard to detect real frequencies above 5 Hz by 30-fps-speed cameras. It is also worth noting that the most recent advances in digital technologies made higher speed (60-120 fps) camera already available at reasonable cost. On the other hand, it is also to be said that most historic structures have their fundamental frequency below 10 Hz, as recent literature on ancient churches [26], towers [27], slender masonry buildings [28] showed. This was confirmed by the recent use of MM and other more conventional methods in archaeological sites [29]. More generally speaking, a recent study on a large set of reinforced concrete (RC) buildings in Europe also found that the fundamental frequency was almost always below 10 Hz [30]. In addition, it is also important to observe that damaged structures tend to reduce their initial fundamental frequency, as structural damage induces stiffness reduction in the materials and in the members' connections [31].

Further limitations in the application of MM methods are related to the physical conditions during video acquisition, such as low or instable lightning conditions, camera instability, improper distance or angle of view from the object, etc. To compensate such limitations several efforts have been lately made to improve the effectiveness of MM algorithms, like the application of Blind Source Separation (BSS) [32] and of several filtering techniques [33].

2.2. Application of the Graph Theory

The Graph Theory (GT) is a relevant mathematical tool that is by now utilised in a wide range of practical applications, such as medicine research, chemistry, genetics, linguistics, and many others. In particular, remarkable potentialities of GT have outstandingly emerged in various fields of engineering. The GT mathematics provide several indices and parameters that have the potentiality to describe the numerous aspects of a process or

a phenomenon, either physical or logical [19], [20]. When GT is used to describe a technological process or a natural phenomenon the graph is typically referred to as a network of nodes or vertices. In general, a graph is defined by a collection of relations connecting its nodes, which are linked by elements, usually referred to as edges. In general, the edges are simple graphic symbols used to indicate that the two linked nodes have some kind of interaction between them, of either mathematical, physical or logical nature, depending on the type of relations we are dealing with. Such relations can be mathematically described by symmetric matrices, usually called adjacency matrices. If a path can be found between any couple of nodes in the network, then the graph is connected.

In the following, we will limit the study to some graph parameters that are expected to be more prone to quantify with a reasonable timing the imminent structural failure of a building during an earthquake shake. The following parameters were considered:

- average degree: defined as the average value of the number of links exiting from a node (also known as node degree) in the network;
- closeness: defined as the sum of the shortest path lengths between a given node and all other nodes in the graph;
- eigenvalue spectra: defined as the eigenvalue of the adjacency matrix A . It can also be computed as the eigenvalue of the Laplacian matrix $L = D - A$, where D is the node degree matrix. The matrix eigenvalues are representative of most of the graph properties;
- spectral gap: this parameter is the difference between the first and second eigenvalue of A . This parameter indicates the network connectivity strength, meaning that it quantifies the robustness of the network connections. It also indicates the presence of bottlenecks, articulation points, or bridges in the network, which is of outmost relevance, because eliminating a bridge can split the network in two or more parts;
- inverse algebraic connectivity: defined as the inverse of the second eigenvalue of the Laplacian in ascending order. The larger the inverse algebraic connectivity, the worse the connectivity, the robustness and the resilience capability of a network [18], [19]. The algebraic connectivity is zero when the graph is not connected, so that the inverse tends to infinite value. In the case of a structure, the network connectivity might be a quantification of the overall integrity of the structure.

Other parameters (e.g. degree distribution, betweenness, clustering etc.) are also commonly utilised to describe specific graph properties, but they require quite larger computational resources and time, especially when the studied graph contains a very large number of nodes. For the above reasons, these parameters were not considered in the present study. In fact, the main objective of this work is to explore the potentialities to extract parameters that can be easily calculated, so that a quasi real-time early warning can be implemented with reasonable computing time.

2.3. Application of the Topological Analysis

Topology offers the basis of a theoretical support to link the GT to the MM method. Since the MM main algorithm is considered as a continuous deformation that keeps the topological properties of the objects, it is reasonable to think of an application to the GT. Until the topological properties hold, the GT allows consistently the calculation of the graph parameters. Even if in the following this aspect will not be treated in detail, it is worth noting that the proposed approach is

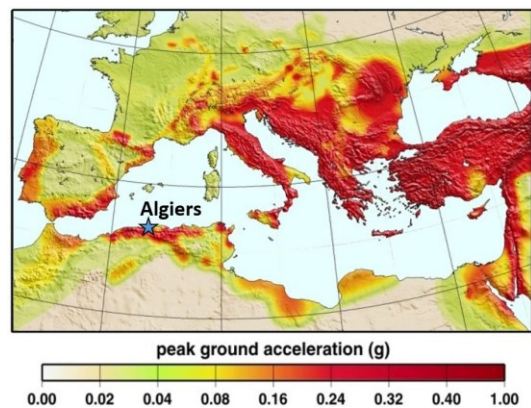


Figure 1. Seismic hazard map of the Mediterranean area with peak ground acceleration (g) for a 90% non-exceedence probability within 50 years. From data in [10].

different from the topological analysis (TA) described in [34] and also from the Graph Signal Processing (GSP) [20], although a common ground between these approaches exists. One of the first uses of the GSP and the graph properties in the vibration analysis of civil structures was proposed in [35]. However, the approach proposed in the present methodology is radically new for the use of video pixels as “virtual sensors”, whereas [35] used clustered MEMS sensors to provide acceleration data.

3. EXPERIMENTAL VALIDATION

3.1. Case study

The present study focused on a typical historic masonry structure that can be found in the Mediterranean area. More specifically, the northern coastal area of Algeria was considered. Here, a strong earthquake (Mw 6.8) struck the coastal region east of Algiers and the Tell Atlas of Algeria on 21 May, 2003. It caused severe damage in historic masonry structures and about 2,400 casualties [36]. The capital city of Algiers is located about 50 km west from the epicentre of the mainshock. In Figure 1 the position of Algiers in the seismic hazard map of the Mediterranean area is illustrated.

The tested mock-up was a full-scale masonry cross vault on the model of the vaults in the private mosque within the Palace of the Dey, also known as Algiers Castle, located inside the Casbah (Citadel) of Algiers. A plan view of the mosque of Dey can be seen in Figure 2.

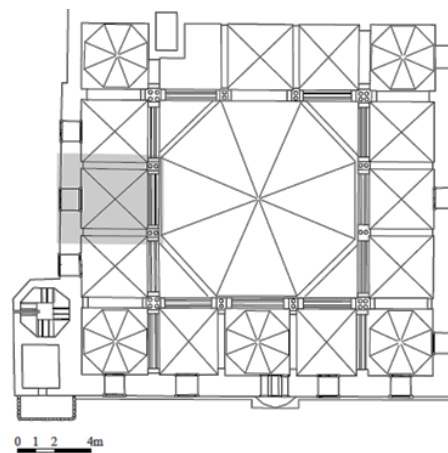


Figure 2. Plan view of the private mosque within the Palace of the Dey, Algiers. The grey area on the left indicates the studied vault.

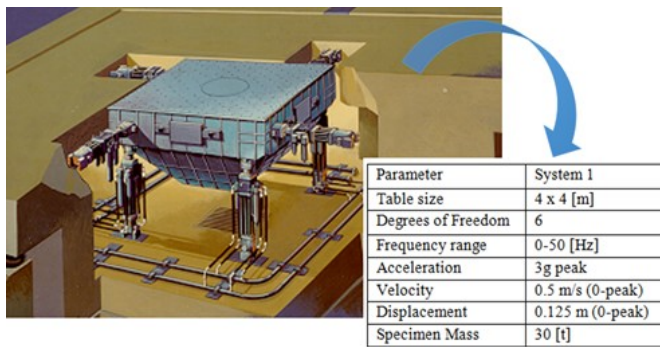


Figure 3. Scheme of System 1 shaking table at ENEA Casaccia research Centre.

It was built as a shelter and headquarter during the Ottoman occupation (16th century), being the Dey the title given to the ruler of the Regency of Algiers under the Ottoman Empire. Unfortunately, archive documentation about the building techniques and materials of the mosque is totally missing. In addition, several restoration works were conducted in the following centuries. No detailed documentation was available on such rehabilitation works either. However, visual inspection of the building suggests that the masonry was built according to traditional techniques with weak mortar joints, similarly to other typical Algerian historic masonry structure of the same time.

Accordingly, the mock-up was built with bricks in baked clay, their size was $0.035 \times 0.12 \times 0.25 \text{ m}^3$, while the mortar joints were about 0.025 m thick.

As for the physical and mechanical properties of the mortar, they were based on the available data from samples taken from similar structures in the Casbah (Citadel) of Algiers.

The mortar samples, which were basically made up of clay, small pieces of bricks, gravel, sand, lime and pozzolana, were subjected to compression and three-point bending tests to determine the main mechanical properties [37].

The overall horizontal dimensions of the tested vault's prototype were $3.50 \times 3.00 \text{ m}^2$ and its height was 2.76 m, including 0.40 m of the base foundation needed to anchor the model to the shaking table. The vault thick was 0.12 m. The mock-up did not consider the effect of the marble columns, in order to avoid their influence on the dynamic response of the vault. In order to reduce the overall weight of the mock-up to 10 t, the back wall of the vault was replaced with stainless-steel diagonal bracing with equivalent stiffness.

More details on the building process of the tested mock-up can be found in [37].

3.2. Experimental setup and instrumentation

The mock-up was tested on shaking table at the ENEA Casaccia Research Centre, located near Rome, Italy. Figure 3 shows a scheme of the utilised shaking table and its main technical characteristics. The mock-up was fixed to the shaking table by anchoring the base foundation through stainless steel plates and bars to fixing elements. Several sensors and instrumentation were located to the measurement point of the structure. In particular, in the following we will focus on the displacement data extracted from markers acquired by a 3D motion capture system, named 3DVision [37] and on the video footages recorded by the cameras integrated with the 3DVision system.

The 3DVision is an optical system for 3D motion measurement through a constellation of near infrared digital (NIR) cameras for data acquisition and synchronized movies. 67

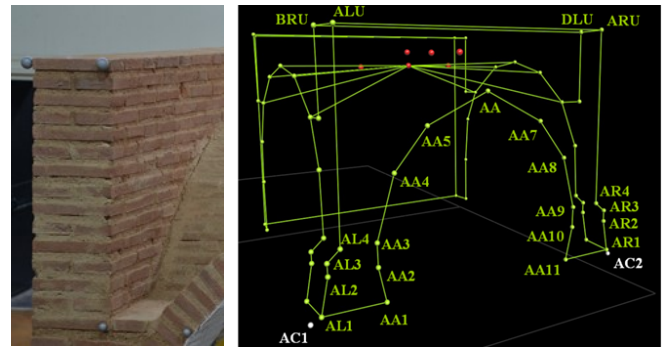


Figure 4. Markers of 3DVision system for displacements measurement (grey balls in the photo on the left). 3D reconstruction of markers positions and nomenclature (right).

retro-reflecting markers were positioned on the tested structure. The markers displacements were reconstructed with accuracy in the order of 0.05 mm in terms of RMS error by spatial triangulation of nine NIR cameras with 3 Mpixel based on Vicon MX technology positioned around the shaking table at a distance of about 5 m from the tested mock-up. The positions and nomenclature of the considered markers can be seen in Figure 4.

The video footages were taken from a distance of about 10 m from the tested mock-up by using a video camera with 656×490 pixel resolution at a frame rate of 30.3 fps.

3.3. Experimental program

The ground motion registered at the Keddara seismic station in North-South direction was the signal provided as input to the shaking table (ked_NS) along the direction transversal to the main façade of the vault. In Figure 5 the ked_NS acceleration time history and spectral response.

The input was scaled in acceleration intensity so as to perform increasing shakes with steps of 0.05 g of Peak Ground Acceleration (PGA). The tested ended with vault collapsed at the shake with 0.25g of PGA (Figure 6).

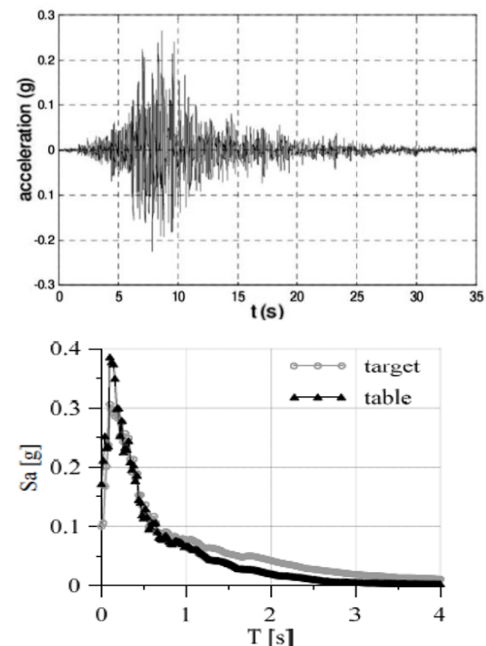


Figure 5. Shaking table seismic input (ked_NS): acceleration time history (top) and acceleration spectral response S_a (bottom).

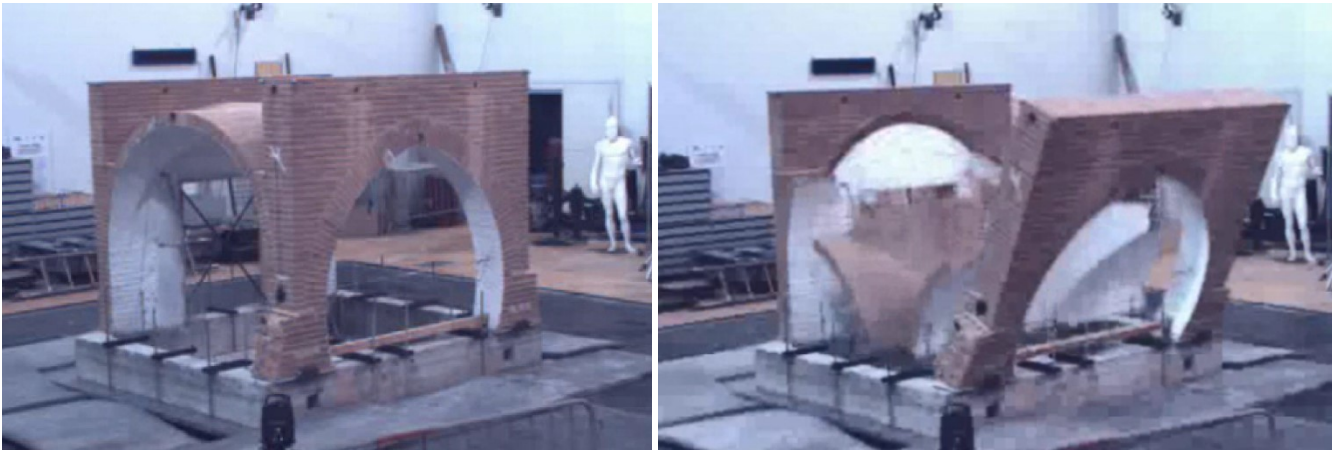


Figure 6. Video footage of the structure during seismic test ked_NS at 0.25 g: before collapse (left) and after complete activation of collapse mechanism (right).

Before and after each seismic test of the sequence a dynamic identification test was also performed through a quasi white-noise vibration signal at 0.05 g of PGA, so as to excite with low energy the fundamental frequency of the tested structure. These dynamic tests were not processed in the proposed methodology, but were considered to assess the damage level of the structure along the seismic test sequence.

4. RESULTS

The model underwent the ked_NS tests with PGA from 0.05 g to 0.20 g without any significant damage. It was observed that the vault was subjected to initial deformations, mainly localized at the level of the wooden logs and associated to an outward movement of the façade. The vault finally collapsed during the last test with a PGA equal to 0.25 g. The main mechanism of collapse was the out-of-plane response of the model and the development of a four-hinge mechanism of the vault (Figure 6). The in-plane deformation was not symmetric mainly because of the prevailing of some limited but not negligible torsional effects. The structure finally was brought to collapse with a very fragile behaviour, i.e. with little visible warning cracks and deformations before the sudden activation of the failure mechanism. This was confirmed by the relative displacement recorded between the markers of the 3DVision, as shown in Figure 7. In particular, the markers displacements remain quite stable until the time at about 4 s of the test at 0.25 g of PGA.

As for the analysis of the videos by the proposed method, the overall number of frames available for analysis before mock-up

collapse in the final test was 182 (about 6 s at 30 fps). The control parameters described in section 2.2 were calculated in search of significant variations suitable to be used as an alert for early warning system.

Two main problems arose. Firstly, the structural deformation could be too small, which meant too small variations in the parameters to be significant. Secondly, it was not easy to transform each frame into a graph.

The first issue was solved by the application of the MM. It amplified enough the tiny displacements in the video, without major topological modifications.

The second issue was addressed creating a graph according to the criterion of the simple “distance” rule:

$$d_{ij} < h, \text{ in frame } k = 1 \dots n, \quad (5)$$

where i and j are the pixels of the studied object in the k -th frame, n is 182 in our case, h is a given threshold, and d is the difference of a given parameter’s intensity values between pixel i and j . If equation 5 is true, then an edge exists between node i and node j of the graph. Albeit simple, the above rule is able to preserve the necessary topological conditions.

Since the threshold h is not known, a maximization criterion of the cost function of the graph parameters was applied to point it out. The considered parameters were calculated for each 182 frames. This meant for each L_k and A_k , giving rise to a time-series for any given parameter. We looked for a significant variation in these time series in relation with the threshold h for each parameter. For example, the results illustrated in Figure 8 show that the inverse algebraic connectivity remained below the

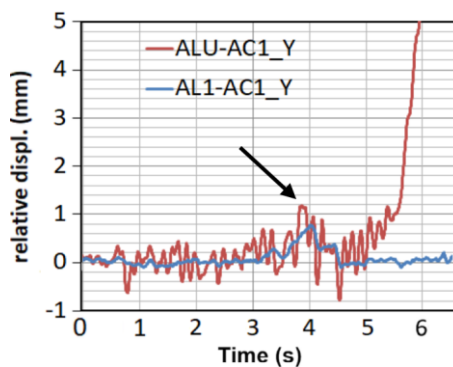


Figure 7. Relative displacement between markers during seismic test ked_NS at 0.25 g. The arrow indicates an anomalous peak before collapse.

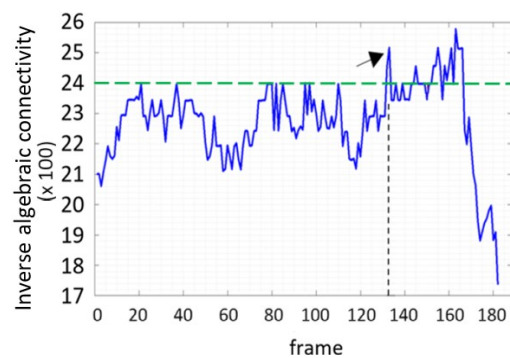


Figure 8. Inverse of the algebraic connectivity. The arrow indicates a peak over the threshold indicated by the green dotted line.

value of 0.024 during the test until time $t = 4.39$ s from test start (corresponding to frame 133 in the magnified video), which is when the seismic test reached the peak acceleration of 0.25 g. The time provided by the above warning signal is approximately confirmed by the contemporary abrupt change in the relative displacements of the markers in Figure 7. In fact, the trend in the relative displacement between markers ALU-AC1 (located at the vault top and foundation, respectively) also gave a threshold value (about 1 mm indicated by the black arrow in Figure 7) that occurred at time equal to about 4 s. The initiation of the final failure can be considered occurring at about 5 s. In particular, at time $t = 5.40$ s (corresponding to frame 163 in the magnified video), the ALU-AC1 relative displacement diverged definitely (i.e. the deformations in the structure became so large because its material had lost its linear elastic behaviour so that the building had lost its load-bearing capacity and was destined to fail). Contemporarily, the inverse algebraic connectivity indicates that the overall shape of the building has changed sufficiently to lose its topological properties, which do not hold anymore. Finally, at time $t = 6.00$ s (frame 182) the collapse was irreversibly activated. Consequently, the value of 0.024 in the inverse algebraic connectivity proved a valid threshold to trigger an alert signal that the network (i.e. the building) is quickly losing connectivity, which means that the structure is rapidly losing rigidity.

5. DISCUSSION

One of the main practical issues of the application of the GT is the creation of a well-defined graph that is representative of the structure. In this context, the extraction of the proper pixels from the video footage is crucial for the algorithm. In fact, clearly not all the pixels are relative to the studied structure and they should not be considered. In particular, in the presented case study the pixels related to objects outside the shaking table should be eliminated from the graph. However, it could be assumed that they remain substantially still and stable during the seismic tests. Consequently, their effect on the graph is invariant if the lighting is perfectly stable, so that they can be easily discarded from the computation process.

Furthermore, in the case of application in the real world, it should be taken into account that the camera is also subjected to the seismic vibration. Consequently, the camera should be fixed in a reliably stable and safe position. However, it is worth remembering that in real application the recorded motion are the relative camera-structure motions, while in the shaking table case study the method was applied to the absolute structural motions. So, in theory, the shaking table testing scenario is more challenging and confusing for the algorithm because the pixels of the structure change significantly according to absolute vibration even when the structure is totally undamaged. On the contrary, in real scenarios, with video recordings of relative movements, the pixels of the structure change significantly only when large relative deformations occur in the structure with comparison to the camera vibration.

Another remarkable open issue is the precise determination of a reliable threshold. It is worth noting that the transformation problem frame-to-graph is transferred to the determination of a correct threshold.

A contribution to this issue can be provided by the possibility of calibrating a predictable threshold by numerical simulations. Calibration and prediction of the structural behaviour of the studied structure through the use of digital twins and numerical

models should be considered to improve to effectiveness and reliability of the proposed method.

From a theoretical point of view, the described methodology is based on the analysis of an N -dimensional time series, where N is the number of considered pixels. These can be mapped onto a time-variant graph, whose topological features can be described by some graph spectral parameters, such as the Fiedler eigenvalue. The high dimensional problem due to the pixel time-series can be reduced by the use of the Laplacian matrix L to a lower dimensional space. In fact, L can be derived directly from a physical representation of the structures, corroborating the choice of using the graph representation as a diagnostic tool. For example, in [38] some details are provided on how to calculate L from the stiffness matrix of a simple mass-spring system, where the Fiedler eigenvalue is the first ortho-normalised mode of vibration of the system. Under the assumption that the system can be considered locally linear, then the following equation can be considered to obtain a good estimate of L :

$$L = \sqrt{\frac{\text{cov}(F)}{\text{cov}(s)}}, \quad (6)$$

where F and s are the force and the displacement covariance matrices respectively, while L is the Laplacian stiffness matrix. Therefore, the Fiedler eigenvalue of L is a proper parameter to describe the dynamic behaviour of the system, as long as the linearity between forces and displacements is still valid.

The first application of the Fiedler eigenvalue to industrial processes was illustrated in [39]. However, the proposed methodology constitutes a substantial new contribution. In fact, it is not only a new application of the above approach to the analysis of video recording technology, but it also adds a new method to point out a calibrated threshold having reasonable timing for a usable imminent collapse early warning system.

6. CONCLUSIONS

In the present study a new methodology for a collapse early warning system based on the application of GT and TA to magnified videos by MM algorithm of a historic structure was explored.

The validation of the proposed methodology was carried out through the application to a laboratory case study. In particular, a destructive shaking table test was performed on a historic masonry full-scale mock-up. The seismic experimentation reproduced the effects of an earthquake occurred in Algeria on an ancient cross vault of the private mosque in the Palace of the Dey, located in the Casbah of Algiers.

The masonry structure was tested until its final collapse. The innovative approach based on topological graph invariants obtained from the MM video was applied to the collapse of the tested structure.

The problems and issues encountered in the transformation of each video frame in a representative graph were outlined and discussed. After determining a reliable graph for the studied structure, some standard graph parameters were calculated and analysed. The choice was made on the least complicated graph parameters from a computational point of view. This was motivated by the need of extracting reliable values in a short timing so as to be used in an effective early warning system.

Among the tested graph parameters, the inverse algebraic connectivity emerged as the one with the most promising potentialities. In fact, experimental results gave a significant early

signal to predict the collapse. In particular, during the seismic test at 0.25 g of PGA, the inverse algebraic connectivity gave values below the threshold of 0.024 as long as the structural integrity was confirmed also by visual inspection and by other instrumentation. The above threshold was exceeded after about 4 s from test start.

This was approximately the same timing as that of a similar signal provided by the relative displacements between the markers of the 3DVision motion capture system indicating anomalous structural deformation in some critical positions of the vault.

In definitive, the found threshold identified through the proposed methodology was validated both by visual evidence and by an independent monitoring system.

Considering that at time equal to about 6 s the collapse mechanism was fully activated, the found threshold gave a warning of almost 2 s in advance. This is not much early warning time for saving lives, but it is enough for interrupting energy lines, for activating fire prevention systems or protection systems for valuable objects and to stop critical machinery.

It is noteworthy that the video camera utilised in the presented experimentation was a quite low-performance (30-fps speed at 656 x 490 pixel resolution) equipment in order to minimise cost.

On the basis of the encouraging results we found, further studies with more accurate data and different experimental cases could be carried out to consolidate the viability of the proposed methodology.

For example, using already available video cameras with 60-fps or even 120-fps speed at Full HD or higher (e.g. 4K, 8K etc.) pixel-resolution, the results might potentially be quite better at a still reasonable cost.

Moreover, it should be also considered that the analysed laboratory case study was conducted in a particularly challenging scenario for the validation of the methodology in terms of structural deformation detection by video footage analysis. Further experiments should consider locating the video camera on the shaking table in a protected position.

In terms of future perspective, further studies will focus on the calibration of the parameters threshold and on a more solid and reliable identification and definition of the graph representative of the structure. Moreover, the algorithms could be improved and optimized in order to minimize the requested computational time, which is particularly crucial to generate an effectively usable early warning signal. In particular, algorithms and data management will have to be optimised for real time processing of video streams, in order to reduce latency and improve collapse anticipation time of the early warning system.

REFERENCES

- [1] G. Grünthal, C. Bosse, S. Sellami, D. Mayer-Rosa, D. Giardini, Compilation of the GSHAP regional seismic hazard for Europe, Africa and the Middle East, *Annali di Geofisica* 42(6) (1999), pp. 1215-1223. DOI: [10.4401/ag-3782](https://doi.org/10.4401/ag-3782)
- [2] C. Scuro, D. L. Carni, F. Lamonaca, R. S. Olivito, G. Milani, Preliminary study of an ancient earthquake-proof construction technique monitoring via an innovative structural health monitoring system, *ACTA IMEKO* 10(1) (2021), pp. 47–56. DOI: [10.21014/acta_imeko.v10i1.819](https://doi.org/10.21014/acta_imeko.v10i1.819)
- [3] I. Roselli, M. Malena, M. Mongelli, N. Cavalagli, M. Gioffrè, G. De Canio, G. de Felice, Structural health monitoring by ambient vibration testing of the “Ponte delle Torri” of Spoleto during the 2016-2017 Central Italy seismic sequence, *Int. J. of Civil Structural Health Monitoring* 8(2) (2018), pp. 199-216. DOI: [10.1007/s13349-018-0268-5](https://doi.org/10.1007/s13349-018-0268-5)
- [4] G. de Alteriis, E. Caputo, R. Schiano Lo Moriello, On the suitability of redundant accelerometers for the implementation of smart oscillation monitoring system: Preliminary assessment, *Acta IMEKO* 12(2) (2023), pp. 1–9. DOI: [10.21014/actaimeko.v12i2.1532](https://doi.org/10.21014/actaimeko.v12i2.1532)
- [5] E. Reynders, System identification methods for (operational) modal analysis: review and comparison, *Archives of Computational Methods in Engineering* 19(1) (2012), pp. 51–124. DOI: [10.1007/s11831-012-9069-x](https://doi.org/10.1007/s11831-012-9069-x)
- [6] I. Roselli, A. Tati, V. Fioriti, I. Bellagamba, M. Mongelli, R. Romano, G. De Canio, M. Barbera, M. Magnani Cianetti, Integrated approach to structural diagnosis by non-destructive techniques: the case of the temple of Minerva Medica, *Acta IMEKO* 7(3) (2018), pp. 13-19. DOI: [10.21014/acta_imeko.v7i3.558](https://doi.org/10.21014/acta_imeko.v7i3.558)
- [7] D. Pellegrini, A. Barontini, M. Girardi, P. B. Lourenço, M. G. Masciotta, N. Mendes, C. Padovani, L. F. Ramos, Effects of temperature variations on the modal properties of masonry structures: An experimental-based numerical modelling approach, *Structures* 53 (2023), pp. 595-613. DOI: [10.1016/j.jstruc.2023.04.080](https://doi.org/10.1016/j.jstruc.2023.04.080)
- [8] R. Azzara, M. Girardi, V. Iafolla, D. M. Lucchesi, C. Padovani, D. Pellegrini, Ambient Vibrations of Age-old Masonry Towers: Results of Long-term Dynamic Monitoring in the Historic Centre of Lucca, *International Journal of Architectural Heritage* 15(1) (2021), pp. 5–21. DOI: [10.1080/15583058.2019.1695155](https://doi.org/10.1080/15583058.2019.1695155)
- [9] A. Sofi, J. Jane Regita, B. Rane, H. H. Lau, Structural health monitoring using wireless smart sensor network – An overview, *Mech. Syst. Signal Process.* 163 (2022), art. no. 108113. DOI: [10.1016/j.ymssp.2021.108113](https://doi.org/10.1016/j.ymssp.2021.108113)
- [10] G. Cosoli, A. Mobili, E. Blasi, F. Tittarelli, M. Martarelli, G. M. Revel, Development and metrological characterization of cement-based elements with self-sensing capabilities for structural health monitoring purposes, *Acta IMEKO* 12(2) (2023), pp. 1 – 12. DOI: [10.21014/actaimeko.v12i2.1420](https://doi.org/10.21014/actaimeko.v12i2.1420)
- [11] P. Baquedano Juliá, T. M. Ferreira, H. Rodrigues, Post-earthquake fire risk assessment of historic urban areas: A scenario-based analysis applied to the Historic City Centre of Leiria, Portugal, *International Journal of Disaster Risk Reduction* 60 (2021), art. no. 102287. DOI: [10.1016/j.ijdrr.2021.102287](https://doi.org/10.1016/j.ijdrr.2021.102287)
- [12] J. Wang, H. You, X. Qi, N. Yang, BIM-based structural health monitoring and early warning for heritage timber structures, *Automation in Construction* 144 (2022), art. no. 104618. DOI: [10.1016/j.autcon.2022.104618](https://doi.org/10.1016/j.autcon.2022.104618)
- [13] Y. M. Wu, H. Kanamori, Development of an earthquake early warning system using real-time strong motion signals, *Sensors* 8(1) (2008), pp. 1-9. DOI: [10.3390/s8010001](https://doi.org/10.3390/s8010001)
- [14] A. Zona, Vision-based vibration monitoring of structures and infrastructures: An overview of recent applications, *Infrastructures* 6(1) (2021). DOI: [10.3390/infrastructures6010004](https://doi.org/10.3390/infrastructures6010004)
- [15] D. C. Kammer, M. L. Tinker, Optimal placement of triaxial accelerometers for modal vibration tests, *Mech. Syst. Signal Process* 18(1) (2004), pp. 29–41. DOI: [10.1016/S0888-3270\(03\)00017-7](https://doi.org/10.1016/S0888-3270(03)00017-7)
- [16] N. Wadhwa, J. G. Chen, J. B. Sellon, D. Wei, M. Rubinstein, R. Ghaffari, D. M. Freeman, O. Büyüköztürk, (+ 3 more authors), Motion microscopy for visualizing and quantifying small motions, *Proc. of Natl. Acad. Sci. USA* 114 (2017) 44, pp. 11639–11644. DOI: [10.1073/pnas.1703715114](https://doi.org/10.1073/pnas.1703715114)
- [17] V. Fioriti, I. Roselli, A. Cataldo, S. Forliti, A. Colucci, M. Baldini, A. Picca, Motion magnification applications for the protection of Italian cultural heritage assets, *Sensors* 22(24) (2022), pp. 9988-

9994.
DOI: [10.3390/s22249988](https://doi.org/10.3390/s22249988)
- [18] G. D'Agostino, A. Scala, *Network of Networks: the last frontier of complexity science*, Springer, 2014, ISBN 978-3319035178.
- [19] M. Newman, *Networks: An Introduction*, Oxford University Press, 2010, ISBN 9780199206650.
DOI: [10.1093/acprof:oso/9780199206650.001.0001](https://doi.org/10.1093/acprof:oso/9780199206650.001.0001)
- [20] D. I. Shuman, S. K. Narang, P. Frossard, A. Ortega, P. Vandergheynst, The emerging field of signal processing on graphs: Extending high-dimensional data analysis to networks and other irregular domains, *IEEE Signal Processing Magazine* 30(3) (2013), pp. 83-98.
DOI: [10.1109/MSP.2012.22235192](https://doi.org/10.1109/MSP.2012.22235192)
- [21] I. Stewart, *Concepts of modern mathematics*, Dover Publication Inc., 1995, ISBN 9780486284248.
- [22] I. Roselli, M. Mongelli, A. Tati, G. De Canio, Analysis of 3D motion data from shaking table tests on a scaled model of Hagia Irene, *Istanbul, Key Engineering Materials* 624(2015), pp. 66-73.
DOI: [10.4028/www.scientific.net/KEM.624.66](https://doi.org/10.4028/www.scientific.net/KEM.624.66)
- [23] H. Y. Wu, M. Rubinstein, E. Shih, J. Gutttag, F. Durand, W. Freeman, Eulerian video magnification for revealing subtle changes in the world, *ACM Trans. Graph.* 31(4) (2012), pp. 1-8.
DOI: [10.1145/2185520.2185561](https://doi.org/10.1145/2185520.2185561)
- [24] N. Wadhwa, M. Rubinstein, F. Durand, W. T. Freeman, Phase-based video motion processing, *ACM Transactions on Graphics* 32(4) (2013), pp. 1-10.
DOI: [10.1145/2461912.2461966](https://doi.org/10.1145/2461912.2461966)
- [25] J. Y. An, S. I. Lee, Phase-based motion magnification for structural vibration monitoring, *IEEE Access* 10 (2022), pp. 123423-123435.
DOI: [10.1109/ACCESS.2022.3224601](https://doi.org/10.1109/ACCESS.2022.3224601)
- [26] S. Lopez, M. D'Amato, L. Ramos, M. Laterza, P. B. Lourenço, Simplified formulations for estimating the main frequencies of ancient masonry churches, *Front. Built Environ.* 5(18) (2019), pp. 1-15.
DOI: [10.3389/fbuil.2019.00018](https://doi.org/10.3389/fbuil.2019.00018)
- [27] A. Montabert, C. Giry, C. Limoge Schraen, J. Lépine, C. Choueiri, E. D. Mercerat, P. Guéguen, An open database to evaluate the fundamental frequency of historical masonry towers through empirical and physics-based formulations, *Buildings* 13(9) (2023), art. no. 2168.
DOI: [10.3390/buildings13092168](https://doi.org/10.3390/buildings13092168)
- [28] M. Shakya, H. Varum, R. Vicente, A. Costa, Empirical formulation for estimating the fundamental frequency of slender masonry structures, *International Journal of Architectural Heritage* 10(1) (2016), pp. 55-66.
DOI: [10.1080/15583058.2014.951796](https://doi.org/10.1080/15583058.2014.951796)
- [29] V. Fioriti, I. Roselli, A. Tati, R. Romano, G. De Canio, Motion magnification analysis for structural monitoring of ancient constructions, *Measurement* 129 (2018), pp. 375-380.
DOI: [10.1016/j.measurement.2018.07.055](https://doi.org/10.1016/j.measurement.2018.07.055)
- [30] M. R. Gallipoli, M. Mucciarelli, B. Šket-Motnikar, P. Zupančić, A. Gosar, S. Prevotnik, M. Herak, J. Stipčević, (+ 3 more author), Empirical estimates of dynamic parameters on a large set of European buildings, *Bull Earthquake Eng* 8 (2010), pp. 593-607.
DOI: [10.1007/s10518-009-9133-6](https://doi.org/10.1007/s10518-009-9133-6)
- [31] G. Hearn, R. B. Testa, Modal analysis for damage detection in structures, *Journal of Structural Engineering* 117(10) (1991), pp. 3042-3063.
- [32] V. Fioriti, I. Roselli, G. De Canio, Modal identification from motion magnification of ancient monuments supported by blind source separation algorithms, *Proc. of COMPDYN 7th ECCOMAS, Crete, Greece, 24-26 June 2019*.
- [33] M. Verma, S. Raman, Edge-aware spatial filtering-based motion magnification. In: Chaudhuri, B., Kankanhalli, M., Raman, B. (eds) *Proceedings of 2nd International Conference on Computer Vision & Image Processing. Advances in Intelligent Systems and Computing* 704 (2018) Springer, Singapore, pp.117-128.
DOI: [10.1007/978-981-10-7898-9_10](https://doi.org/10.1007/978-981-10-7898-9_10)
- [34] T. Gowdrige, N. Dervilis, K. Worden, On topological data analysis for structural dynamics: An introduction to persistent homology, *ASME Open J. Engineering*. January 2022 1 011038.
DOI: [10.1115/1.4055184](https://doi.org/10.1115/1.4055184)
- [35] F. Zonzini, A. Girolami, L. De Marchi, A. Marzani, D. Brunelli, Cluster based vibration analysis of structure with SGP, *IEEE Trans. Ind. El.*, 68(4) (2020), pp. 3465-3474.
DOI: [10.1109/TIE.2020.2979563](https://doi.org/10.1109/TIE.2020.2979563)
- [36] H. Bechtoula, H. Ousalem, The 21 May 2003 Zemmouri (Algeria) Earthquake: damages and disaster responses, *Journal of Advanced Concrete Technology* 3(1) (2005), pp. 161-174.
DOI: [10.3151/jact.3.161](https://doi.org/10.3151/jact.3.161)
- [37] M. Rossi, C. Calderini, I. Roselli, M. L. Mongelli, G. De Canio, S. Lagomarsino, Seismic analysis of a masonry cross vault through shaking table tests, *Earthquakes and Structures* 18(1) (2020), pp. 57-72.
DOI: [10.12989/eas.2020.18.1.057](https://doi.org/10.12989/eas.2020.18.1.057)
- [38] E. Gutiérrez Tenreiro, F. Bono, C. Coutsomitros, Data analysis of non-standard time series: The role of graph Laplacians and covariance matrices in data and processes and complex systems, *EUR 28191 EN. Luxembourg (Luxembourg): Publications Office of the European Union; 2016. JRC103730*.
DOI: [10.2788/1139](https://doi.org/10.2788/1139)
- [39] M. S. Tootooni, P. K. Rao, C. A. Chou, Z. J. Kong, Spectral graph theoretic approach for monitoring times series data from complex dynamical processes, *IEEE Trans. Aut. Sci. Eng.* 15(1) (2018), pp. 127-144.
DOI: [10.1109/TASE.2016.2598094](https://doi.org/10.1109/TASE.2016.2598094)